

Thermal evolution of neutron stars with global and local neutrality

S. M. de Carvalho^{1,2}, R. Negreiros², Jorge A. Rueda^{1,3,4}, Remo Ruffini^{1,3,4}

¹*ICRANet-Rio, Centro Brasileiro de Pesquisas Físicas,*

Rua Dr. Xavier Sigaud 150, Rio de Janeiro, RJ, 22290-180, Brazil

²*Instituto de Física, Universidade Federal Fluminense, UFF, Niterói, 24210-346, RJ, Brazil*

³*Dipartimento di Fisica and ICRA, Sapienza Università di Roma, P.le Aldo Moro 5, I-00185 Rome, Italy and*

⁴*ICRANet, P.zza della Repubblica 10, I-65122 Pescara, Italy*

(Dated: November 20, 2014)

Globally neutral neutron stars, obtained from the solution of the called Einstein-Maxwell-Thomas-Fermi equations that account for all the fundamental interactions, have been recently introduced. These configurations have a more general character than the ones obtained with the traditional Tolman-Oppenheimer-Volkoff, which impose the condition of local charge neutrality. The resulting configurations have a less massive and thinner crust, leading to a new mass-radius relation. Signatures of this new structure of the neutron star on the thermal evolution might be a potential test for this theory. We compute the cooling curves by integrating numerically the energy balance and transport equations in general relativity, for globally neutral neutron stars with crusts of different masses and sizes, according to this theory for different core-crust transition interfaces. We compare and contrast our study with known results for local charge neutrality. We found a new behavior for the relaxation time, depending upon the density at the base of the crust, ρ_{crust} . In particular, we find that the traditional increase of the relaxation time with the crust thickness holds only for configurations whose density of the base of the crust is greater than $\approx 5 \times 10^{13} \text{ g cm}^{-3}$. The reason for this is that neutron star crusts with very thin or absent inner crust have some neutrino emission process blocked which keep the crust hotter for longer times. Therefore, accurate observations of the thermal relaxation phase of neutron stars might give crucial information on the core-crust transition which may aid us in probing the inner composition/structure of these objects.

Keywords: Neutron star cooling; neutrino emission.

I. INTRODUCTION

In recent works [1–4] a new approach has been developed in which a neutron star is considered to have global rather than local charge neutrality. It was shown that the new equilibrium equations, the Einstein-Maxwell-Thomas-Fermi (EMTF) equations, introduce self-consistently the presence of the electromagnetic interactions in addition to the strong, weak, and gravitational interactions, all within the framework of general relativity. The weak interactions are introduced by the β -stability, and the strong interactions are modeled via the σ - ω - ρ nuclear model. In this work we adopt the NL3 parameterization of this nuclear model [see 3, and references therein for more details]. The supranuclear core is composed by a degenerate gas of neutrons, protons, and electrons. The crust, in its outer region ($\rho \leq \rho_{\text{drip}} \approx 4.3 \times 10^{11} \text{ g cm}^{-3}$), is composed of ions and electrons, while in its inner region ($\rho_{\text{drip}} < \rho < \rho_{\text{nuc}}$, where $\rho_{\text{nuc}} \approx 2.7 \times 10^{14} \text{ g cm}^{-3}$ is the nuclear saturation density), there is an additional component of free neutrons dripped out from nuclei.

The solution of the EMTF equations leads to a new structure of neutron stars, significantly different from the traditional configurations obtained through the TOV equations (see Fig. 1): the core is positively charged due to gravito-polarization, giving rise to a Coulomb potential energy, $eV \sim m_{\pi}c^2$. The core-crust transition takes place at the nuclear saturation density $\rho = \rho_{\text{nuc}}$. The transition is signaled by the existence of a thin

($\Delta r \sim \text{few hundreds fm}$) electron layer, fully screening the core charge. In this transition layer the electric field becomes overcritical, $E \sim (m_{\pi}/m_e)E_c$ with $E_c = m_e^2 c^3 / (e\hbar)$ the critical field for vacuum polarization, and the particle densities decrease until the base of the crust, which is reached when global charge neutrality is achieved. Consequently, the density at the base of the crust is characterized by $\rho_{\text{crust}} \leq \rho_{\text{nuc}}$. Furthermore due to the appearance of an electric field, the core-crust transition is no longer contiguous, since as discussed above there is now a gap with width Δr filled by the screening electrons.

Configurations with $\rho_{\text{crust}} > \rho_{\text{drip}}$ possess both inner and outer crust, whereas in the cases with $\rho_{\text{crust}} \leq \rho_{\text{drip}}$ the neutron star has only an outer crust. In the limit $\rho_{\text{crust}} \rightarrow \rho_{\text{nuc}}$, both Δr and E of the transition layer vanish, and the solution approaches the one given by local charge neutrality (see Figs. 3 and 5 in [3]). Details on the boundary and equilibrium conditions leading to these configurations are presented below in the next section. All the above features lead to a new mass-radius relation of neutron stars as shown in Fig. 2; see [3] for further details.

The aim of this work is to compute the thermal evolution of globally neutral neutron stars for different values of the density of the crust, ρ_{crust} , covering configurations with and without inner crust, all the way to the limit $\rho_{\text{crust}} \approx \rho_{\text{nuc}}$, which corresponds to TOV-like solutions satisfying local charge neutrality. The article is organized as follows. We discuss in section II gravito-polarization

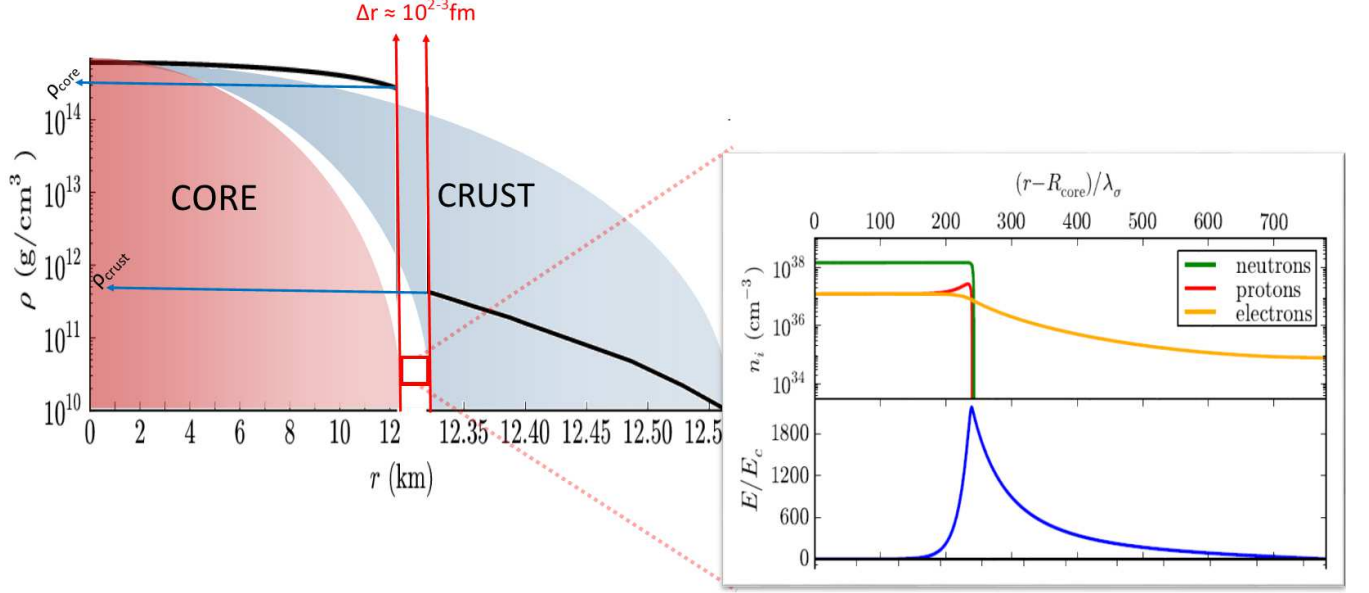


FIG. 1. In the top and center panels we show the neutron, proton, electron densities and the electric field in units of the critical electric field E_c in the core-crust transition layer, whereas in the bottom panel we show a specific example of a density profile inside a neutron star. In this plot we have used for the globally neutral case a density at the edge of the crust equal to the neutron drip density, $\rho_{\text{drip}} \approx 4.3 \times 10^{11} \text{ g cm}^{-3}$, and $\lambda_\sigma = \hbar/(m_\sigma c) \sim 0.4 \text{ fm}$ denotes the σ -meson Compton wavelength.

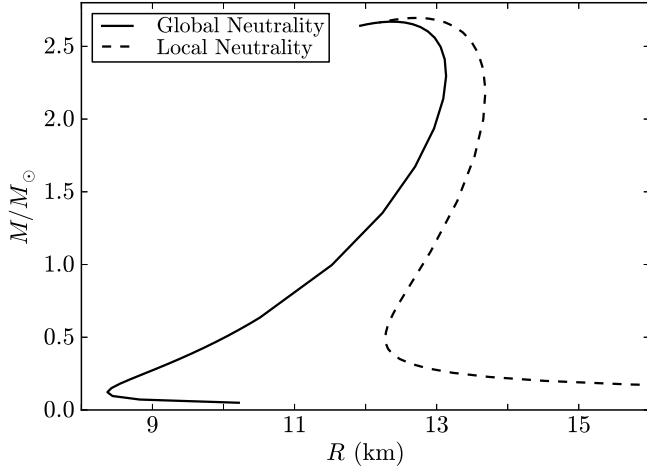


FIG. 2. Mass-radius relation obtained with the traditional locally neutral TOV treatment case and the global charge neutrality configurations, with $\rho_{\text{crust}} = \rho_{\text{drip}}$ [3]. Configurations lying between the solid and dashed curves have $\rho_{\text{crust}} > \rho_{\text{drip}}$ and so they possess inner crust.

effects in neutron stars and the boundary conditions of neutron stars satisfying global charge neutrality. In section III we recall the equations of thermal evolution in the spherically symmetric case and the cooling mechanisms taken into account in this work. We show in section IV the cooling curves obtained from the numerical integration of the thermal evolution equations and compute the thermal relaxation time of the configurations. The ef-

fects of pairing effects in the crust in the cooling curves are shown in section V and we finally summarize our conclusions in section VI. We use geometric units $G = c = 1$ throughout the article.

II. CORE-CRUST TRANSITION AND FAMILY OF GLOBALLY NEUTRAL SOLUTIONS

The specific value of ρ_{crust} establishes the properties of the core-crust transition surface as follows. The matching of the core to the crust is at $r = R_{\text{core}} + \Delta r$. The equilibrium conditions are given by the constancy of the particle Klein potentials (or generalized Fermi energies) throughout the configuration

$$E_i^F = e^{\nu(r)/2} \mu_i(r) + \mathcal{V}_i(r) = \text{constant}, \quad (1)$$

where μ_i and \mathcal{V}_i are the free-chemical potential and effective potentials of the i -specie. \mathcal{V}_i includes the electromagnetic and nuclear potentials. $e^{\nu(r)}$ is the 0-0 component of the spherically symmetric metric

$$ds^2 = e^{\nu(r)} dt^2 - \frac{dr^2}{1 - 2m(r)/r} - r^2 d\theta^2 - r^2 \sin^2 \theta d\varphi^2, \quad (2)$$

with r the radial coordinate and $m(r)$ is the mass function.

The matter in the crust is thought to be solid-like composed of an electron-ionic lattice at densities $\rho \leq \rho_{\text{drip}}$ and by an electron-neutron-ionic lattice at $\rho > \rho_{\text{drip}}$. The description of the matter can be simplified by the

introduction of Wigner-Seitz cells: each cell contains a central ion of total positive charge $+eZ$ (Z denotes the number of protons), surrounded by compressed degenerate cloud of relativistic electrons which fully screened the ion positive charge at the cell's border (i.e. number of electrons in the cell equal to Z). At densities higher than the neutron-drip value, there is present also the background of neutrons. The equation of state of matter in such a state of high density and pressure was first computed in a classic work by Baym, Bethe and Pethick [5]. The distribution of electrons around each nucleus is assumed to be uniform and the nuclear model was based on a phenomenological extension of the semi-empirical liquid-drop model which allows nuclear compressibility. It was also included the reduction of the nuclear surface tension in presence of the neutron background for densities higher than the neutron-drip value. The effect of inhomogeneities in the electron distribution around the nucleus was recently examined in [6] by extending the classic Thomas-Fermi model to relativistic regimes and introducing the nucleus finite size. The extension to finite temperatures of that treatment was recently presented in [7]. The electron density, so computed, takes into account self-consistently both the electron-electron and electron-ion Coulomb interactions. The equilibrium configuration of the electrons is characterized by higher values close to the nucleus surface and decreases outwards until it fully screens the ion at the Wigner-Seitz cell's radius.

The Wigner-Seitz cells, which are globally neutral, can be thought as the building blocks of the crust. The equilibrium distribution of such neutral cells in the crust is then expected to occur without gravito-polarization, and therefore no net electric field, Coulomb potential, and charge should appear. On the contrary, in the neutron star core, charge separation occurs since charged particles (proton and electrons) are 'free' to flow, gravitationally segregating. Indeed, as shown in Eq. (21) in [1], the Coulomb potential depth at the center of the core is proportional to the proton-electron mass difference, i.e. $eV(r=0) \propto (m_p - m_e)c^2$. Hence, a transition from a charged region (the core) to a neutral region (the crust), has to be present in the system.

For the electron gas, the Eq. (1) imposes, in the transition layer, the following continuity condition

$$E_e^F = e^{\nu_{\text{core}}/2} \mu_e^{\text{core}} - eV^{\text{core}} = e^{\nu_{\text{crust}}/2} \mu_e^{\text{crust}}, \quad (3)$$

where $\mu_e^{\text{core}} = \mu_e(R_{\text{core}})$, $eV^{\text{core}} = eV(R_{\text{core}})$, and $\mu_e^{\text{crust}} = \mu_e(R_{\text{core}} + \Delta r)$, and $e^{\nu_{\text{crust}}} \simeq e^{\nu_{\text{core}}}$, with the effective potential for the electrons $\mathcal{V}_e = -eV$, namely the electron Coulomb potential energy (since electrons are blind to the strong force).

We have used in Eq. (3) the fact that no Coulomb potential appears in the crust and our previous results which show that the transition occurs at distance-scales $\Delta r \sim \hbar/(m_e c) \ll R_{\text{core}}$, leading to a negligible gradient of the gravitational potential in such a region. This equation tells us that the Coulomb potential gap created between the charged core and the crust is of

the order of $\Delta eV \sim \Delta \mu_e = \mu_e^{\text{core}} - \mu_e^{\text{crust}}$, which for $\mu_e^{\text{crust}} \ll \mu_e^{\text{core}}$ becomes of the order of $m_\pi c^2$ [1]. Under such conditions, there is an electric field in the transition $E \sim \Delta V/\Delta r \sim (m_\pi/m_e)E_c$.

In the transition region both the electron chemical potential and the density decrease (see Fig. 1), namely $\mu_e^{\text{crust}} < \mu_e^{\text{core}}$ and $\rho_{\text{crust}} < \rho_{\text{core}}$. The electron chemical potential at the base of the crust μ_e^{crust} is an increasing function of the crust base density ρ_{crust} . Hence, for increasing values of ρ_{crust} the Coulomb potential gap is reduced leading to lower values of the electric field in the interface. The properties of this interface, such as its surface energy, the electric field, and the consequent Coulomb energy, were recently explored in [8] up to the limit of locally neutral configurations for which ρ_{crust} is close to the nuclear saturation value. It was there shown how (see, e.g., Fig. 4 in that reference), indeed, the Coulomb energy is a decreasing function of the crust matching density, ρ_{crust} .

All the above implies that for each central density, a family of core-crust interfaces exists. Correspondingly, for a given central density, there is an entire family of crusts with different mass and thickness. We analyze below the thermal evolution of neutron stars for different values of the crust density ρ_{crust} , all the way up to approaching the limit of locally neutral configurations, which occurs for $\mu_e^{\text{crust}} \rightarrow \mu_e^{\text{core}}$, namely when $\rho_{\text{crust}} \rightarrow \rho_{\text{nuc}}$, approximately.

It is worth mentioning before closing this section, for the sake of completeness, scenarios in which the sharp transition becomes smoother. First of all let us briefly discuss the case in which the crust is in a fluid-like state. It is clear, following the above discussion, that in such a case the Wigner-Seitz cell construction does not apply any longer and macroscopic gravito-polarization effects, owing to gravitational segregation of the ions, should appear. This would change the afore discussed core-crust boundary matching conditions with consequences on the interface properties, likely reducing the interfacial electric field. This would lead to a smoother transition and the star would possibly develop a Coulomb potential and an electric field from the center all the way up the surface.

In addition, we would like to recall the consequences of requesting that more than one charge is conserved (e.g. baryon and electric) within the Gibbs construction of the thermodynamic phase-transition. This case leads to the appearance of "mixed-phases" in between of the pure homogeneous phases, where essentially the two phases coexist, one over a background formed by the other, and in which a non-vanishing electric charge must exist forming charged Wigner-Seitz cells. Therefore, also in this case only the global charge neutrality of the system can be imposed (see, Refs. [9–14], for further details). The equilibrium pressure of the phases varies with the density creating a spatially extended and smoother phase-transition region of non-negligible thickness with respect to the star radius and without any density jump. However, the homogeneous pure phases in these treat-

ments are still subjected to the condition of local charge neutrality, and so they do not account for the possible presence of interior Coulomb fields caused by gravitopolarization, as previously discussed.

III. THERMAL EVOLUTION EQUATIONS

The general relativistic equations of energy balance and energy transport for the description of the thermal evolution, in the spherically symmetric case treated here, read [see e.g. 15–17]

$$\frac{\partial(Le^\nu)}{\partial r} = -\frac{4\pi r^2}{\sqrt{1-2m/r}} \left[\epsilon_\nu e^\nu + c_\nu \frac{\partial(Te^{\nu/2})}{\partial t} \right], \quad (4)$$

$$\frac{Le^\nu}{4\pi r^2 \kappa} = \sqrt{1-2m/r} \frac{\partial(Te^{\nu/2})}{\partial r}. \quad (5)$$

Eqs. (4–5) depend on the structure of the star through the variables r , $m(r)$, $\rho(r)$, and $\nu(r)$ that represent the radial distance, the mass function, the energy density, the general relativistic gravitational potential, respectively. The thermal variables are represented by the interior temperature $T(r, t)$, the luminosity $L(r, t)$, neutrino emissivity $\epsilon_\nu(r, T)$, thermal conductivity $\kappa(r, T)$ and specific heat per unit volume $c_\nu(r, T)$.

The boundary conditions of Eqs. (4–5) are determined by the luminosity at the center and at the surface. The luminosity vanishes at the stellar center, i.e. $L(r=0)=0$, since at this point the heat flux is zero. At the surface, the luminosity is defined by the relationship between the mantle temperature, which we denote to as T_b , and the temperature outside of the star, $T(r=R)=T_s$ [18–21].

As for the thermal processes taken into account, in the core we consider the direct¹ and modified Urca processes, and the Bremsstrahlung process among the nucleons. In the crust we have plasmon decay, e^-e^+ pair annihilation, electron-nucleus and electron-nuclei Bremsstrahlung. Heat capacity and thermal conductivity follow their traditional formulation as described in [20] and references therein.

It is important to notice that pairing effects are extremely important for the cooling of a neutron stars [see e.g. 22, 23, for a recent study of the effects of pairing in the thermal evolution of compact stars]. However, for the purposes of this work, that is to investigate the thermal properties of globally neutral neutron stars with relation to their possible different crust thickness, we focus our attention in the case in which pairing effects are “turned off”, as to obtain a better comprehension of the effects of the crust thickness to the cooling. For the sake of completeness we will perform a preliminary study in which

we consider a conservative scheme for neutron and proton pairing. Clearly, once we obtain a better comprehension of the thermal evolution of globally neutral neutron stars we intend to augment this study by including more sophisticated processes, such as more sophisticated pairing and rotation effects [24, 25]

IV. COOLING CURVES AND THERMAL RELAXATION TIME

We turn now to the general properties of the cooling curves of globally neutral neutron stars. Exploring the freedom allowed by the global charge neutrality approach (namely the value of ρ_{crust}), we investigate the thermal evolution of stars with different structures. Each neutron star study has the same gravitational mass ($M \approx 1.4 M_\odot$) with different values for ρ_{crust} , which in turn is reflected in the thickness of the crust. In other words the core of these objects are largely the same, their crust, however, are increasingly thinner for smaller values of the density at its base, ρ_{crust} . This is illustrated in Fig. 3. We note that the configuration whose $\rho_{\text{crust}} = 2.4 \times 10^{14} \text{ g cm}^{-3}$ has approximately the structure of a locally neutral neutron star, so this configuration should exhibit traditional cooling properties known in the literature.

We computed the cooling curves by integrating numerically the energy balance and transport equations (4–5) for the configurations shown in Fig. 3.

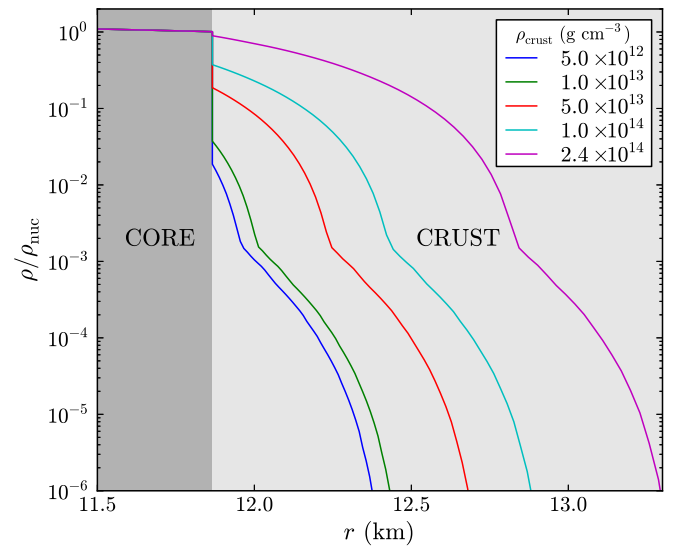


FIG. 3. Density profiles of globally neutral neutron star with mass $M \approx 1.4 M_\odot$ for selected values of the density at the base of the crust, ρ_{crust} . Notice that at the transition, the density of the core is that of the nuclear saturation density, ρ_{nuc} .

¹ Allowed by energy-momentum conservation only if the particle fraction satisfies the triangle inequality $P_n^F < P_p^F + P_e^F$, where $P_{n,p,e}^F$ are the Fermi momenta of neutrons, protons, and electrons, respectively.

In Fig. 4 we show the surface temperature as observed at infinity, as a function of time t in yr for the neutron star configurations shown in Fig. 3.

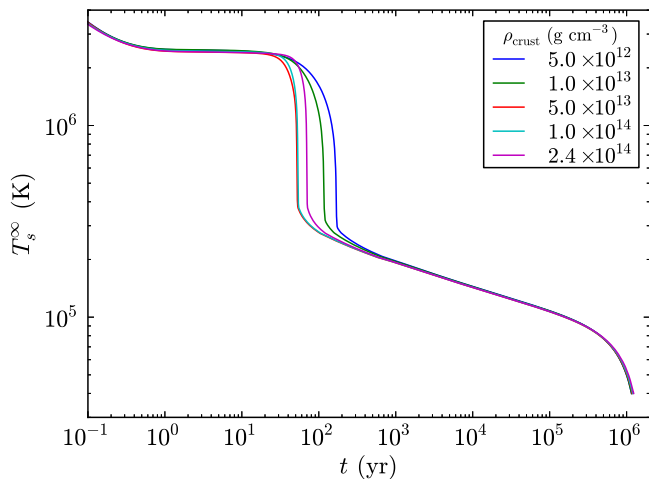


FIG. 4. Surface temperature at infinity T_s^∞ as a function of time t in yr for the neutron star configurations shown in Fig. 3.

Fig. 4 shows us that the different configurations have qualitatively the same behavior. However, the thermal relaxation time, t_w [26], of each is different. This quantity is defined as the time at which the star becomes isothermal. Such time is signaled by a temperature drop in the surface temperature. The intensity of such drop will depend on whether or not fast neutrino processes (such as the DU) are taking place in the core. For stars younger than $t = t_w$, the crust of the star is hotter than the core and so heat flows from the crust to the core, or equivalently as a cooling front propagating from the core to the crust. The time t_w is therefore the time it takes for cooling front to reach the star surface.

For traditional neutron stars, namely under the assumption of local charge neutrality, [27] it is found by numerical simulations that t_w is longer for thicker crusts, following approximately $t_w \propto \Delta R_{\text{crust}}^{1.4-1.8}$, where ΔR_{crust} is the crust thickness. The Fig. 5 is an enlargement of Fig. 4 around the temperature drop at the end of the thermal relaxation phase. As illustrated in Fig. 4, we see that for the neutron stars we are studying, the aforementioned behavior is only valid for stars whose $\rho_{\text{crust}} \geq 5 \times 10^{13} \text{ g cm}^{-3}$. For stars with $\rho_{\text{crust}} \leq 5 \times 10^{13} \text{ g cm}^{-3}$, however, we observe the opposite behavior, that is, an increase in t_w for thinner crusts. In order to understand such behavior we need to realize two things: 1: The thickness of the crust contributes to increase t_w , since for a thicker crust the cooling front needs to “travel” a larger distance; and 2: For crusts with larger ρ_{crust} we have more intense emission of neutrinos from the crustal region. In the case of traditional neutron stars the range of densities covered by the crust is roughly the same, thus if the crust thickness is reduced one naturally obtains a smaller t_w (since the crustal neutrino emission stays the same while the crust is thinner). In our study however, we consider different crust thickness and ρ_{crust} , thus while initially (when the variation of ρ_{crust} is small)

the crustal neutrino emission is roughly the same (while the thickness is reduced), we have the reduction of t_w (as in traditional neutron stars). However, when ρ_{crust} is significantly reduced, the neutrino emitting region is also significantly reduced. Therefore, we have two competing processes: the increase of t_w due to the reduction of neutrino emission and the decrease of t_w due to the geometrical reduction of the crust thickness. We have found that for $\rho_{\text{crust}} \lesssim 5 \times 10^{13} \text{ g cm}^{-3}$ the former wins and we have an overall increase of t_w for such stars.

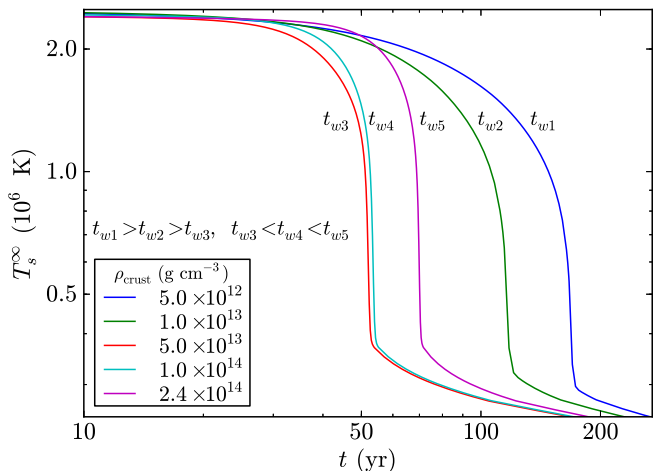


FIG. 5. Enlargement of the evolution of the surface temperature around its drop at the end of the thermal relaxation phase, for the neutron stars shown in Fig. 3.

V. PAIRING EFFECTS

For completeness we have also considered pairing in the interior of neutron star. As mentioned before, neutron and proton pairing is fundamental for the temperature evolution of the object. In this study, with the intention of not deviating from the main goal (i.e. the investigation of the core-crust transition in the thermal evolution) we chose a conservative pairing scheme, in which we have neutron singlet (1S_0) pairing in the crust (for the regions above neutron drip density), neutron triplet (3P_2) pairing and proton singlet (1S_0) pairing for the core region. We notice that in our conservative approach we do not have pairing extending to high densities regions of the core.

We summarize our results in Fig. 6, where the thermal evolution of neutron stars with proton and neutron pairing is compared to the results previously discussed. For this analysis we have only used the two extreme core-crust transitions, with all the other results lying in between. As illustrated in Fig. 6 the inclusion of pairing has its traditional effect of slowing the thermal evolution of the star, although the objects with different core-crust configurations exhibit, qualitatively, the same behavior as discussed before.

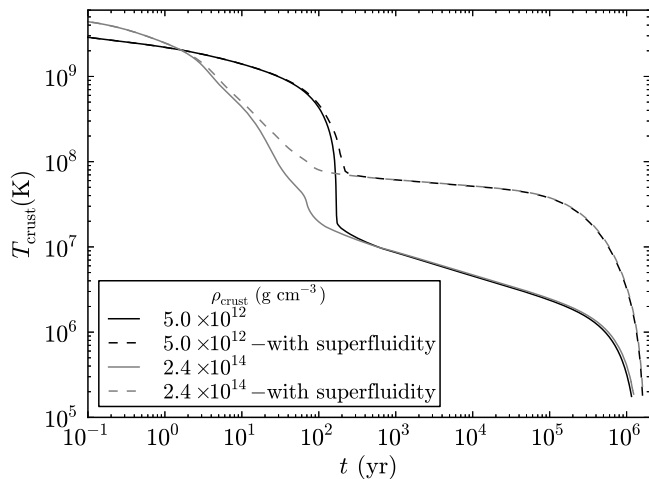


FIG. 6. Same as in Fig. 4 but for neutron stars with proton and neutron pairing.

VI. DISCUSSION

In this work we have investigated the thermal properties of neutron stars satisfying global, rather than local, charge neutrality conditions. Within this model one no longer has a contiguous transition from the core to the crust of the neutron star. Instead there is gap ($\Delta R \sim 10^2\text{--}3\text{fm}$) filled by a distribution of electrons and an ultra-high electric field. Under this description the density at the base of the crust might be as low as the neutron drip density, which means that one may obtain neutron stars with very different crusts: thin for the models whose density at the crust base is low; or thick in the case of larger values of the crust base density; all the way to the limit of local charge neutrality (where there is a continuous transition from core to crust). Evidently the question of which description (thicker or thinner crust) arises. Since the crust plays a small role in the the mass of the neutron star, and the fact that observation of the radii are still far from coming to reality, we resort to the thermal evolution of neutron stars to obtain hints on how to constrain the crust thickness.

We have shown that the structure of the neutron stars satisfying global charge neutrality may potentially lead to specific signatures in the thermal evolution of the neutron star. In particular, it has been shown that the traditional proportionality between the relaxation time and

the crust thickness is violated for stars whose densities at the crust base is lower than $\approx 5 \times 10^{13} \text{ g cm}^{-3}$, in which case the opposite behavior occurs, namely one obtains a longer relaxation time for thinner crust. The reason for this is the reduction of the crustal neutrino emission (due to the overall reduction of the crust density), which contributes to keeping the crust warm, compensating the speed up even though the reduction of the crust size tend to speed up cooling. It is important to notice that for densities higher than this value the traditional behavior is restored, in which the relaxation time increases with the crust thickness. These subtle effects are potentially observable in the thermal relaxation phase of the neutron star, which however has been observationally evasive until now. The observations of this early evolution of the neutron star might therefore probe the properties of the core-crust transition and thus may aid us in testing the underlying theory of global charge neutrality. We also call the attention to the fact that in the case in which the density at the base of the crust is equal to the neutron drip density ($\rho_{\text{drip}} \approx 4.3 \times 10^{11} \text{ g cm}^{-3}$), we have a situation that is similar to that of quark stars. Such hypothetical objects are composed of absolutely stable quark matter, and thus, due to charge neutrality at the surface of the quark core an ultra-high electric field arises filling the region between the core and a thin crust made up of ordinary matter, much like in the model describe in this work. Due to the similarities between these two models it is interesting to investigate and compare the cooling behavior of compact objects described by each model. Such studies are currently under way.

ACKNOWLEDGMENTS

We would like to thank the anonymous referee for the important suggestions which helped us to improve the presentation of our results. S.M.C. acknowledges the support given by the International Relativistic Astrophysics PhD Program through the Erasmus Mundus Grant 2010–1816 from EACEA of the European Commission, during which part of this work was developed. S.M.C. and J.A.R. also acknowledge the support by the International Cooperation Program CAPES-ICRANet financed by CAPES – Brazilian Federal Agency for Support and Evaluation of Graduate Education within the Ministry of Education of Brazil. R. N. acknowledges financial support by FAPERJ and CNPq.

References

-
- [1] M. Rotondo, J. A. Rueda, R. Ruffini, and S.-S. Xue, Phys. Lett. B **701**, 667 (2011).
 - [2] J. A. Rueda, R. Ruffini, and S.-S. Xue, Nucl. Phys. A **872**, 286 (2011).
 - [3] R. Belvedere, D. Pugliese, J. A. Rueda, R. Ruffini, and S.-S. Xue, Nucl. Phys. A **883**, 1 (2012).
 - [4] R. Belvedere, K. Boshkayev, J. A. Rueda, and R. Ruffini, Nucl. Phys. A **921**, 33 (2014), 1307.2836.
 - [5] G. Baym, H. A. Bethe, and C. J. Pethick, Nucl. Phys. A **175**, 225 (1971).
 - [6] M. Rotondo, J. A. Rueda, R. Ruffini, and S.-S. Xue, Phys. Rev. C **83**, 045805 (2011).

- [7] S. M. de Carvalho, M. Rotondo, J. A. Rueda, and R. Ruffini, *Phys. Rev. C* **89**, 015801 (2014).
- [8] J. A. Rueda, R. Ruffini, Y.-B. Wu, and S.-S. Xue, *Phys. Rev. C* **89**, 035804 (2014).
- [9] N. K. Glendenning, *Phys. Rev. D* **46**, 1274 (1992).
- [10] N. K. Glendenning and S. Pei, *Phys. Rev. C* **52**, 2250 (1995).
- [11] M. B. Christiansen and N. K. Glendenning, *Phys. Rev. C* **56**, 2858 (1997).
- [12] N. K. Glendenning and J. Schaffner-Bielich, *Phys. Rev. C* **60**, 025803 (1999).
- [13] M. B. Christiansen, N. K. Glendenning, and J. Schaffner-Bielich, *Phys. Rev. C* **62**, 025804 (2000).
- [14] N. K. Glendenning, *Phys. Rep.* **342**, 393 (2001).
- [15] K. S. Thorne, *Astrophys. J.* **212**, 825 (1977).
- [16] D. Page, U. Geppert, and F. Weber, *Nuclear Physics A* **777**, 497 (2006).
- [17] S. Tsuruta and A. G. W. Cameron, *Nature* **207**, 364 (1965), ISSN 0028-0836, URL <http://www.nature.com/doi/10.1038/207364a0>.
- [18] D. Page, J. M. Lattimer, M. Prakash, and A. W. Steiner, *The Astrophysical Journal Supplement Series* **155**, 623 (2004), ISSN 0067-0049, URL <http://stacks.iop.org/0067-0049/155/i=2/a=623>.
- [19] A. Potekhin, G. Chabrier, and D. Yakovlev, *Arxiv preprint astro-ph/9706148* **428**, 415 (1997), URL <http://arxiv.org/abs/astro-ph/9706148>.
- [20] D. Yakovlev and C. Pethick, *Annual Review of Astronomy and Astrophysics* **42**, 169 (2004), ISSN 0066-4146, 0402143, URL <http://arjournals.annualreviews.org/doi/abs/10.1146/annurev>
- [21] D. Page, J. M. Lattimer, M. Prakash, and A. W. Steiner, *The Astrophysical Journal* **707**, 1131 (2009), ISSN 0004-637X, URL <http://stacks.iop.org/0004-637X/707/i=2/a=1131?key=crossref>
- [22] D. Page, M. Prakash, J.M. Lattimer, and A.W. Steiner, *Physical Review Letters* **106**, 081101 (2011), ISSN 0031-9007, URL <http://link.aps.org/doi/10.1103/PhysRevLett.106.081101>.
- [23] D. G. Yakovlev, W. C. G. Ho, P. S. Shternin, C. O. Heinke, and A. Y. Potekhin, *Monthly Notices of the Royal Astronomical Society* **411**, 1977 (2011), ISSN 00358711, URL <http://doi.wiley.com/10.1111/j.1365-2966.2010.17827.x>.
- [24] R. Negreiros, S. Schramm, and F. Weber, *Phys. Rev. D* **85**, 104019 (2012), 1201.2381.
- [25] R. Negreiros, S. Schramm, and F. Weber, *Physics Letters B* **718**, 1176 (2013), 1103.3870.
- [26] O. Y. Gnedin, D. G. Yakovlev, and A. Y. Potekhin, *MNRAS* **324**, 725 (2001), arXiv:astro-ph/0012306.
- [27] J. M. Lattimer, K. A. van Riper, M. Prakash, and M. Prakash, *Astrophys. J.* **425**, 802 (1994).

